SPACE TELESCOPE SCIENCE INSTITUTE
Operated for NASA by AURA

Instrument Science Report WFC3 2003-06

Masking Technique on WFC3 IR Images

B. Hilbert, S. Baggett, M. Robberto
July 9, 2003

ABSTRACT

This document presents a summary of the strategy used to create mask files for WFC3 IR ground test images. Data from the IR detector is unique in that it is collected in "multi-accum" mode, i.e. a ramp of non-destructive readouts collected for each observation. This provides information on the signal rate in each pixel over the course of the observation, allowing application of a more sophisticated technique to identify bad pixels.

Introduction

In the multiaccum method of data acquisition used in the WFC3-IR channel, each ramp of data is composed of a number of non-destructive reads. As a result, it is possible to monitor the rate of signal generation in each pixel of the detector. Cosmic ray events are then identified by searching for anomalous signal changes across the reads of a given ramp. Depending on the magnitude of the anomaly, and on the stability of the detector, different methods can be used to identify spurious events, and possibly correct the ramps.

In this document, we describe two methods. They have been implemented in IDL and applied on data taken at the Detector Characterization Laboratory (DCL) at Goddard Space Flight Center (GSFC) on the infrared detectors FPA32, FPA45, FPA50, and FPA58. FPA32, and to a lesser extent, FPA58, are relatively stable and straightforward to mask. FPA45 and FPA50 are highly unstable detectors, making effective masking a challenging task: one needs to move away from the method of iterative sigma-clipping in order to identify bad pixels. In this traditional method of masking, all pixels with values outside a given threshold from the mean are marked as bad. The remaining pixels are then used to calculate a new mean and threshold, and the process is repeated. We show that this

method is not effective at identifying all cosmic ray events on those WFC3 IR FPAs that exhibit instabilities in their dark current. Instead, we have developed a 4-step method capable of removing all bad pixels and increasing the accuracy of subsequent calculations.

Masking Procedure

Our method used for producing masks for WFC3-IR data consists of four steps. The first step involves the identification and repair of "glitches" in the data. The remaining steps identify bad pixels through comparisons with the mean and standard deviation of the entire pixel population.

Step One: De-glitching

The first step in creating a suitable mask for WFC3-IR data is a preliminary correction that needs to be applied to the raw data, in order to make the subsequent masking more effective. This correction step involves the identification and repair of sporadic "glitches" seen in the data, that can be attributed to cosmic rays. A plot of the signal in a pixel affected by one of these glitches is shown in Figure 1. The signal is initially collected at a fairly constant rate. The glitch then appears as a sudden jump between two consecutive reads, followed by a return to the initial rate. In WFC3-IR ground-based data, glitches can have a wide range of intensity. They can be very small and in certain cases, even negative, with the pixel suddenly losing some amount of accumulated signal between consecutive reads. In several test cases, the jumps were small enough that they were not identified through traditional masking methods such as sigma-clipping, or the new masking method described in the following sections. Therefore, special steps need to be taken in order to identify and fix them.

We identify glitches through an iterative algorithm. First, the rate of signal generation for a given pixel is found using all the reads of the ramp. All points falling more than a given distance from the mean signal rate are identified. The point with the largest discrepancy from the mean is treated first. If it is a cosmic ray event, all reads subsequent to the corresponding read will have systematically either too much, or too little signal. Using the mean signal rate (from all reads except that containing the glitch), the signals of these post-glitch reads can be corrected to where they would have been without the glitch. An updated mean signal rate for the pixel over the entire ramp is then calculated, and a secondary correction to the post-glitch signal levels is made. This is due to the fact that the initial correction was made based on a mean signal level which included the glitch. The process is then repeated on the same pixel with the new signals, until the signal rate between each read is within the specified distance from the mean. To date, no pixel has yet been observed with more than one glitch per ramp. The results of the correction can be seen again in Figure 1.

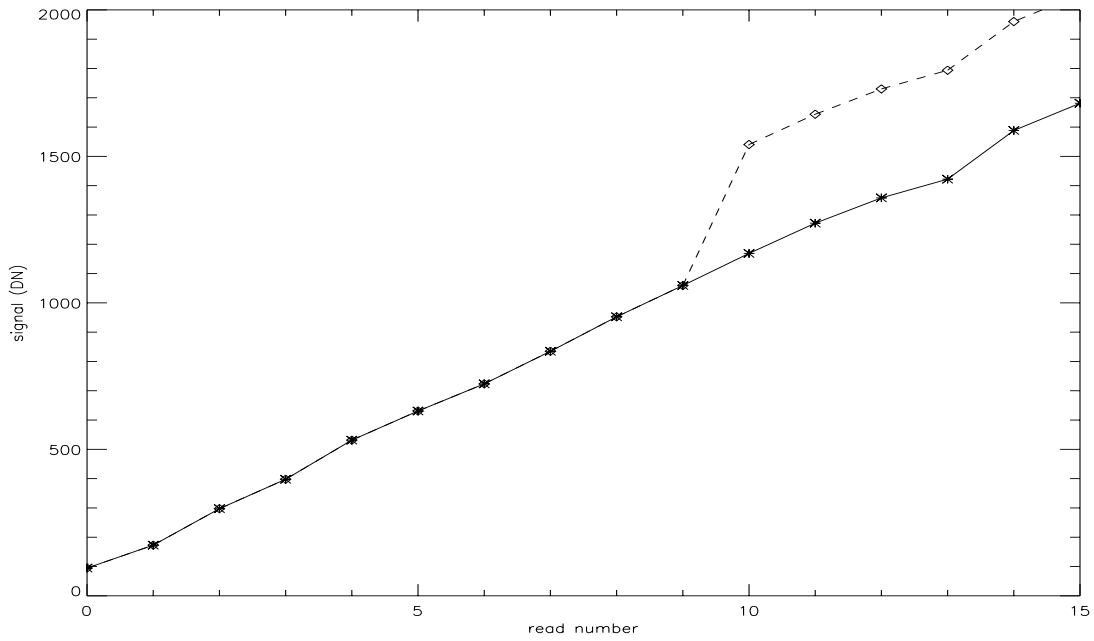

Figure 1: Measured signal of a single pixel through 17 reads of a single ramp. Note the glitch in the data between reads 9 and 10. The dashed line after read 9 shows the original pixel signal. The solid line is the signal in the pixel after the de-glitching process has been applied.

It has been suggested that the glitches are the results of cosmic rays impinging on the electronics rather than the detector itself (Offenberg et al. 2001). If the problem originated as spurious bit changes in the ADC, we would expect the glitch spectrum to show peaks around counts spaced roughly by 2^n values. However this is not the case, as the glitch spectrum shows a single peak at ~100 ADU, as seen in Figure 2.

Future Improvement of the De-glitching Process

The de-glitching process described above has been used with success for a number of focal plane arrays. Development of the algorithm took place using data from FPA45, which is one of the most unstable IR detectors tested at the DCL. On the 1024 x 1024 dark current images examined and corrected for glitches, roughly 1500 pixels were identified as suffering from a glitch in a 20 minute exposure.

A potential problem with the correction method described above became apparent when looking at glitches with large amplitudes. FPA45, along with some of the other FPAs, is known to become unstable when exposed to bright light. More intense light causes a more intense, longer-lasting instability, or persistence, in the detector. The largest glitches observed were in fact large enough to trigger the instability in FPA45. In the reads following a large glitch, an instability was observed, with the signal rate becoming

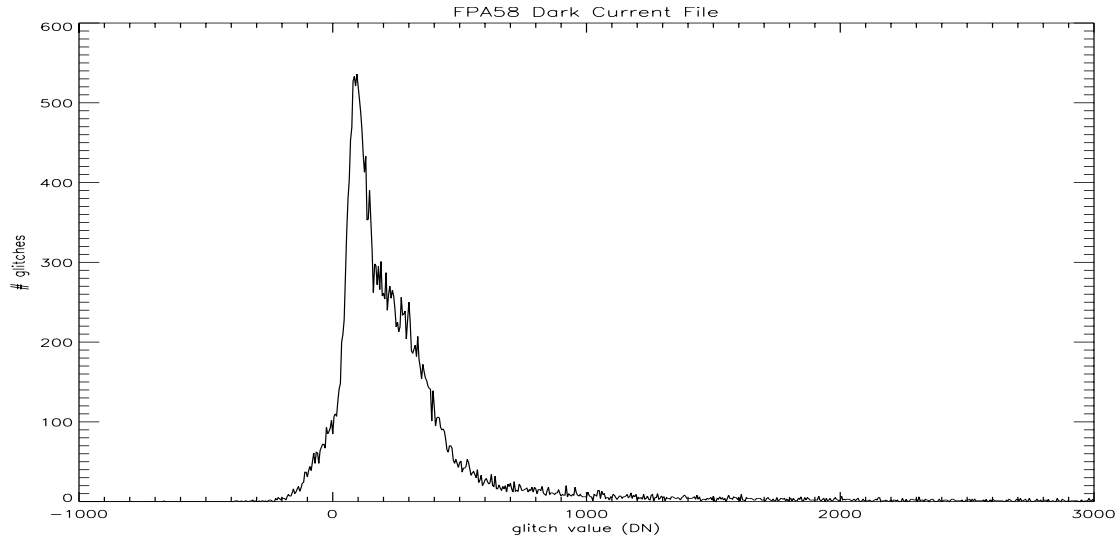

Figure 2: Histogram of the glitch values for one ramp of FPA45 data. The single, broad peak suggests that the source of the glitches is not a problem with the ADC.

negative for a short while before gradually returning to normal. Using the correction method described above on these large glitches results in the glitch itself being removed, but the after-effects of the glitch remain, as seen in Figure 3. The instability, that appears as a negative dark current, remains after the correction. For detectors affected by this anomaly, future versions of the de-glitching technique should take this into account, at least by marking as bad those pixels with glitches large enough to trigger the instability.

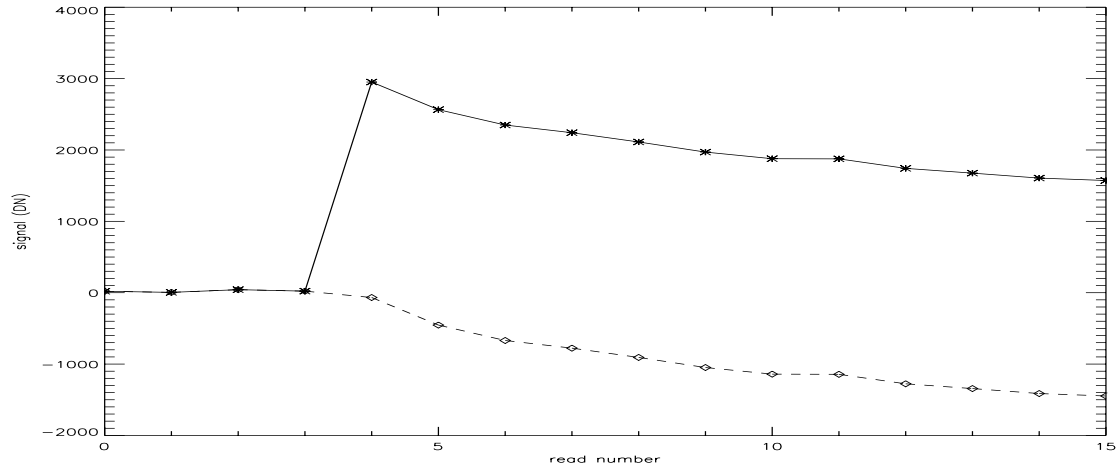

Figure 3: Large glitch, displaying the instability of the detector. The original signal is the solid line, showing a negative signal rate after the glitch. This negative rate remains after the glitch has been repaired (dashed line).

Despite the fact that glitches only affect a small fraction of the total pixels, they appear to have a significant effect on measurements such as dark current and readnoise. Figures 5, 6 and 7 below show the results of dark current and readnoise measures, respectively, comparing non-de-glitched to de-glitched data.

Steps Two Through Four: Bad Pixel Identification

Once the glitches have been removed from a ramp, a 3-step bad pixel identification process is used to create the mask. The method is similar to the traditional method of sigma-clipping used to identify outlying pixels, but variations from sigma-clipping are used to exploit the fact that each observation is composed of a number of non-destructive reads (Don Hall, personal communication).

The mask is created from a pair of dark current ramps, each composed of 16 non-destructive reads, using a 3-step process, where each step creates a partial mask. The three partial masks are then combined to create the final mask.

The first partial mask is created by examining the first read from each of a pair of ramps. These reads are first summed. The mean and standard deviation of the resulting image are calculated. All pixels in the summed image falling outside of a specified threshold from the mean (typically 5σ) are then flagged as bad. This step identifies pixels on the detector that are shorted or unbonded (i.e. a “cold mask”).

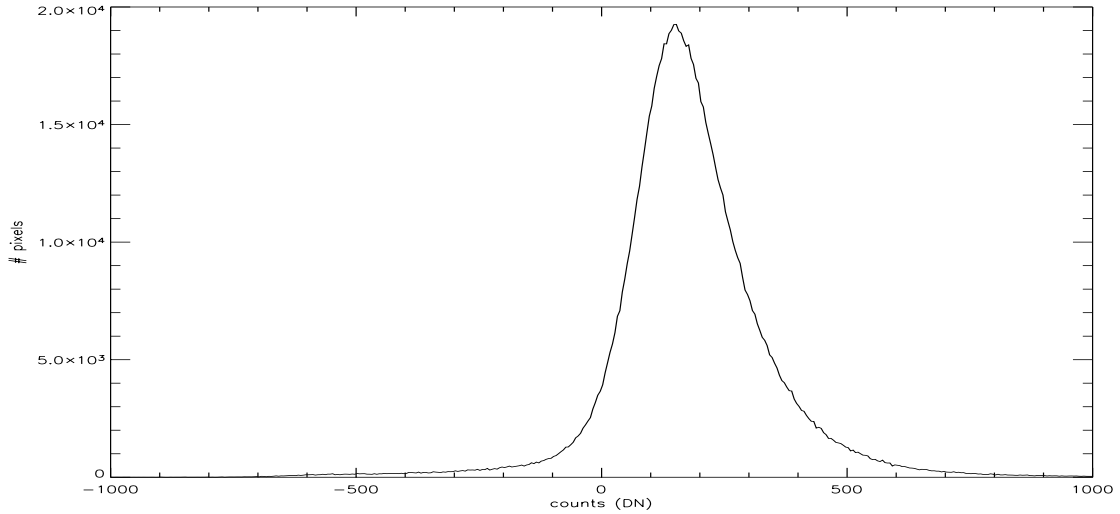

Figure 4: Histogram of the sum of the first reads of two ramps. Bad pixels in the first partial mask are identified by calculating the mean and standard deviation of this distribution. All pixels farther than a given threshold from the mean are marked as bad.

The second partial mask is designed to isolate pixels that have high dark current (i.e. a “hot mask”). Given two ramps, A and B, each of which has 16 reads, the image to be examined in this step is created by adding the read #1 - read #16 double correlated differences.

$$FinalImage = ((A[1] + B[1]) - (A[16] + B[16]))$$

The mean of this final image is calculated and, as in step 1, all pixels falling farther than a given threshold from the mean are considered bad.

The final partial mask is created from a final image similar to that in step 2. This final step is used to identify pixels that, over the course of the two ramps being investigated, exhibit odd behavior, such as from cosmic ray hits. These pixels are not intrinsically bad, but are flagged as bad in order to improve the accuracy of the observation. Our preliminary deglitching procedure should have already corrected these pixels, but this step is included to make the procedure more general. The final image in this case is created by subtracting the read #1 - read #16 double correlated differences. An identical clipping technique to the first two masks is applied in order to identify bad pixels.

$$FinalImage = (A[1] - B[1]) - (A[16] - B[16])$$

Once the three partial masks have been created, they are combined. Any pixel flagged as bad in any of the masks is marked as bad in the composite mask. In addition, any pixel found to be bad is marked as bad in every read of both ramps. Due to the unstable nature of many of the WFC3 FPAs, the overall percentage of bad pixels found varies, but is usually 3%-5%.

The masks resulting from a pair of dark frames are then applied to illuminated images as part of the basic calibration steps prior to analysis of the images. Ideally, the bad pixel populations from masks 1 and 2 should be stable. However, the bad pixel population from mask 3 will vary over time, as it is composed of cosmic ray events and other transient effects. This suggests that masks should only be applied to data files taken close in time to the dark current files used to produce the mask.

Results

In order to study the effectiveness of this new masking method as compared to sigma-clipping, several comparison studies were undertaken. First, the calculation of dark current for FPA58 was performed. Figure 5 shows the quadrant-averaged measured dark current for several ramps of a persistence test dataset with iterative sigma-clipping used to create the mask. Figure 6 shows the same calculation with the new method described above. Clearly, the sigma-clipping masking routine is not as effective at removing bad

pixels as the new masking method. The sigma-clipping routine gave results with a much higher noise component than the de-glitching + 3-step masking technique.

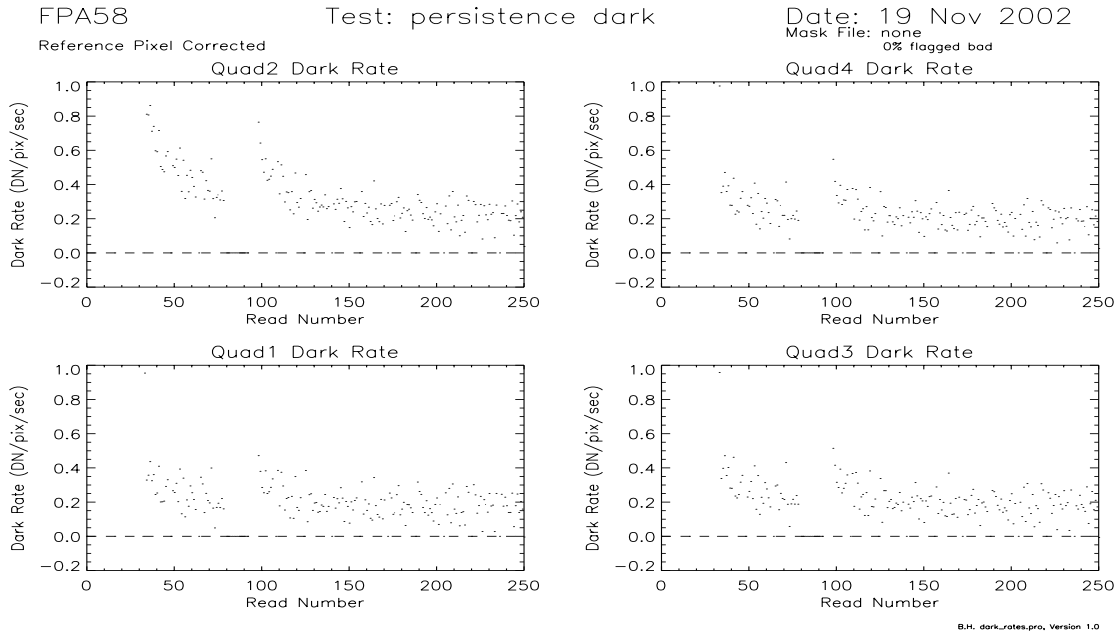

Figure 5: Quadrant-averaged dark rate for the four quadrants of FPA58, using iterative sigma-clipping to produce a mask. Compare the large scatter in the dark rate to that in Figure 6, where the data was de-glitched and masked using the new, 3-step method.

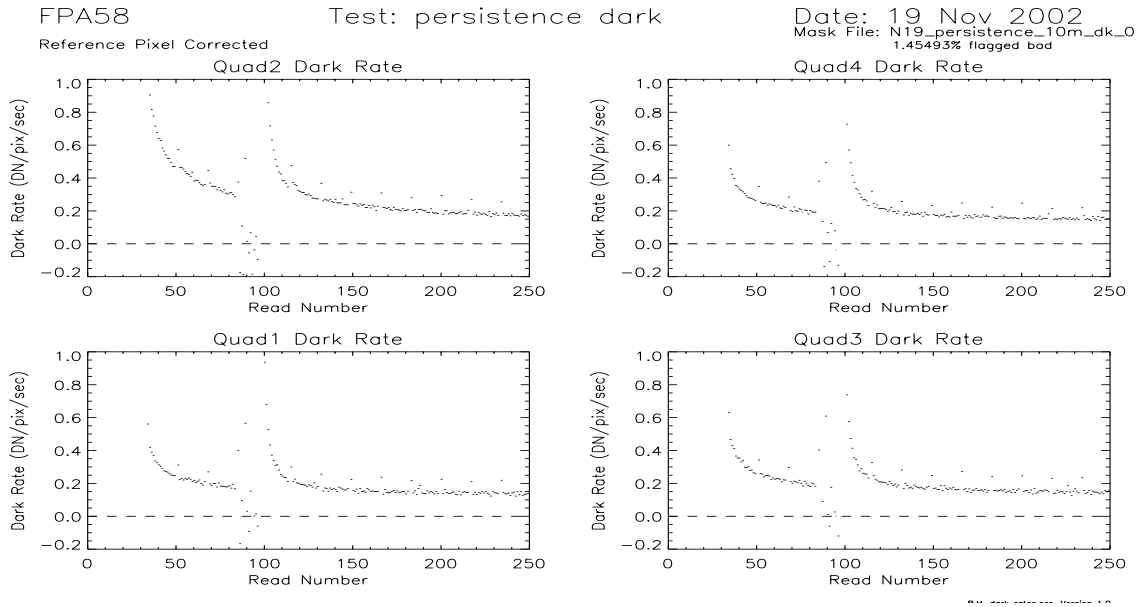

Figure 6: Same data as Figure 5, but de-glitched and masked using the 3-step method. The overall exponential decay of the dark rate is due to instability in the detector.

Also, the readnoise of FPA58, calculated using many small (20 x 20 pixel) areas covering the science area of quadrant 1, was computed using the two masking techniques. Results can be seen in Figure 7. The upper panels of Figure 7 show the readnoise computed from data masked using the iterative sigma clipping technique. The upper left panel uses the second and third readouts of the test data, while the upper right panel uses the fourth and fifth readouts. The lower panels show the readnoise for the same 20 x 20 pixel boxes on the same data, where the de-glitching and new masking processes have been applied. There is clearly a reduction in the scatter of the readnoise measurements in the lower panels, implying that the latter method of masking was more effective at identifying bad pixels.

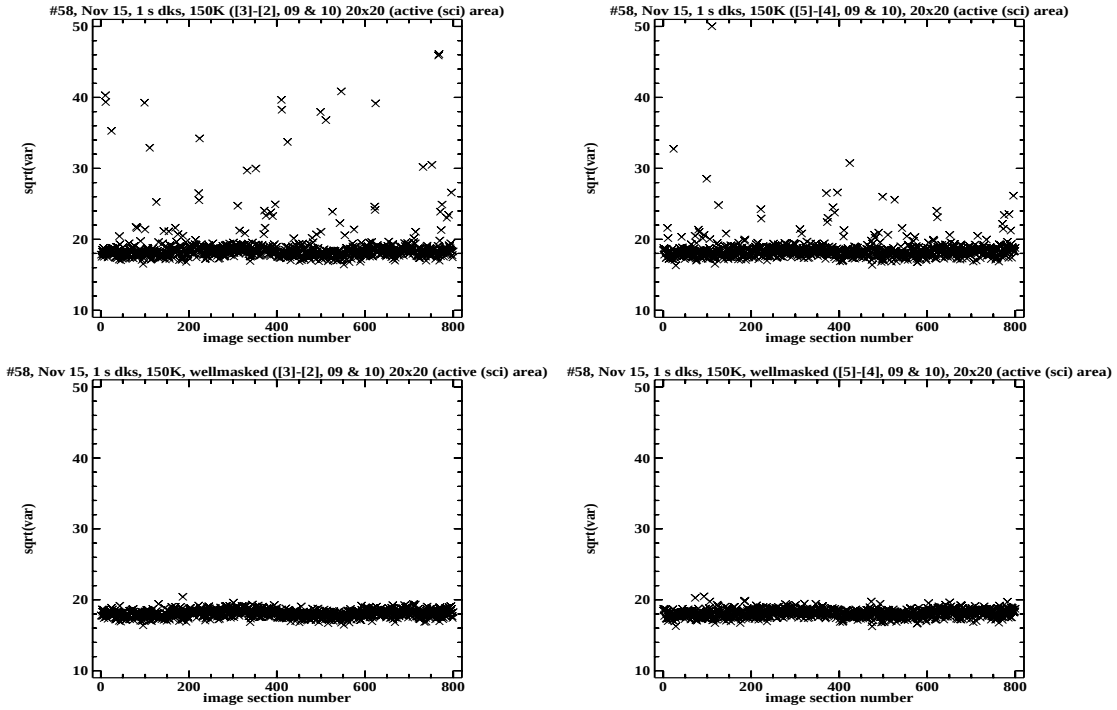

Figure 7: Readnoise calculations on FPA58 data. Each ‘X’ corresponds to the readnoise calculated from one 20x20 pixel box. The upper panels use iterative sigma-clipping for masking, while the bottom panels use de-glitching and the new masking technique.

Conclusions

After de-glitching in order to correct for jumps in signal, a 3-step masking method appears to provide superior results when compared to the more traditional iterative sigma-clipping method of mask production. While sigma-clipping blindly marks bad pixels in each frame regardless of the behavior of those pixels in previous and subsequent frames, the 3-step method of determining bad pixels exploits the multiple-non-destructive reads property of WFC3-IR data, in order to produce a more complete picture of each pixel’s

behavior. As a result, our masking strategy appears to substantially improve the overall reliability of the statistical estimates.

References

Offenberg, J.D., Fixsen, D.J., Rauscher B.J., Forrest, W.J., Hanisch, R.J., Mather, J.C., McKelvey, M.E., McMurray Jr., R.E., Nieto-Santisteban, M.A., Pipher, J.L., Sengupta, R., Stockman, H.S. *Validation of Up-the-Ramp Sampling with Cosmic-Ray Rejection on Infrared Detectors.* **PASP**, 113, p.240, 2001.